Optimization of microwave-assisted polycondensation for flexible biodegradable polyurethane in sustainable packaging applications

Abiodun Abdulhameed Amusa [a,b], Nur Izzati Mohd Razali [c], Fathilah Ali [b,*] [ID],
Tuan Noor Maznee Tuan Ismail [d] [ID], Azlin Suhaida Azmi [b], Jamarosliza Jamaluddin [e]

[a] School of Materials & Mineral Resources Engineering, Universiti Sains Malaysia, 14300, Nibong Tebal, Pulau Pinang, Malaysia
[b] Department of Chemical Engineering and Sustainability, Kulliyyah of Engineering, International Islamic University Malaysia (IIUM), Jalan Gombak, Kuala Lumpur 53100, Malaysia
[c] Department of Biotechnology Engineering, Kulliyyah of Engineering, International Islamic University Malaysia (IIUM), Jalan Gombak, Kuala Lumpur 53100, Malaysia
[d] Advanced Oleochemical Technology Division, Malaysian Palm Oil Board, No. 6, Persiaran Institusi, Bandar Baru Bangi, Kajang, Selangor 43000, Malaysia
[e] Department of Bioprocess and Polymer Engineering, School of Chemical and Energy Engineering, Faculty of Engineering, Universiti Teknologi Malaysia, Johor Bahru, Johor 81310, Malaysia

ARTICLE INFO

ABSTRACT

The proliferation of plastic waste presents a significant environmental challenge due to its persistence and ecological impact. This study explores biodegradable polyurethanes (PUs) as a sustainable packaging alternative, optimizing the microwave-assisted synthesis of polylactic acid (PLA)–diol from palm oil polyol and PLA under varying microwave power (500–700 W) and reaction times (30–45 minutes). Structural characterization was performed with proton Nuclear Magnetic Resonance (^{1}H–NMR) and Fourier Transform Infrared Spectroscopy (FTIR). Mechanical, thermal, and surface properties were investigated using tensile testing, Differential Scanning Calorimetry (DSC), and Scanning Electron Microscopy (SEM). Over 100 days of biodegradation studies were conducted to evaluate their environmental impact. Structural analysis confirmed PLA–diol formation with 92 % yield and a molecular weight (M_n) of 2500 g/mol under optimal conditions (700 W, 45 minutes), compared to 85 % yield and 2000 g/mol at 500 W for 30 minutes. FTIR analysis revealed characteristic absorptions at 3500 cm^{-1} (–OH) and 1750 cm^{-1} (–C$=$O), while ^{1}H–NMR confirmed key signals at 1.58 ppm and 5.16 ppm. Among synthesized PUs, toluene diisocyanate (PU–TDI) exhibited the highest tensile strength (2.90 MPa). In contrast, hexamethylene diisocyanate (PU–HDI) showed superior flexibility with 144.5 % elongation at break and superior thermal stability (melting temperature of 131°C). Biodegradation studies revealed that PU–HDI degraded by 28 % over 100 days, with SEM confirming significant surface erosion. These results demonstrate the potential of optimized biodegradable PUs to address plastic waste challenges and advance sustainable packaging solutions.

1. Introduction

The global surge in plastic waste significantly contributes to the accumulation of waste in landfills and marine ecosystems. Annually, global production of plastics exceeds 300 million tons, with packaging accounting for approximately 40 % of this demand. These materials, characterized by degradation times spanning centuries, present significant challenges to environmental sustainability. Their persistence disrupts ecosystems, facilitates the proliferation of microplastics, and exacerbates greenhouse gas emissions. Consequently, there has been increasing interest in biopolymers derived from renewable resources,

particularly those capable of natural degradation over time [1,2]. Biodegradable polyurethanes (PUs) have gained prominence due to their exceptional strength, flexibility, chemical resistance, and mechanical properties. Additionally, their degradation under suitable conditions yields harmless byproducts, thus reducing pollution and mitigating landfill leachates [3]. These attributes have driven the adoption of PUs across various industries, including automotive, construction, and packaging.

Biodegradable PUs are synthesized using polylactic acid (PLA) as a key precursor with polyols that provide essential hydroxyl (–OH) groups. Typically, these bio–based polyols offer a sustainable alternative

to petroleum-derived materials [4]. PLA is a bioplastic obtained from renewable sources such as corn starch, sugarcane, or cassava, and is widely recognized for its biodegradability, biocompatibility, and relatively low production cost. These characteristics make PLA particularly suitable for packaging applications. However, PLA has intrinsic limitations, such as poor thermal stability, brittleness, and low elongation at break, which restricts its use in applications requiring flexibility and durability. Additionally, PLA's hydrophilic nature compromises its performance in moist environments, and its slow degradation under ambient conditions raises concerns for specific practical applications [5]. To address these limitations, blending PLA with other materials has emerged as a viable strategy to enhance its properties while maintaining its biodegradability.

One promising additive is palm oil polyol, a sustainable and renewable alternative to petroleum–based polyols. Chemically modified from palm oil, this polyol is particularly advantageous due to its natural abundance in palm oil-producing regions and its functionality conferred by its –OH groups. Incorporating palm oil polyol into PLA–based systems mitigates brittleness and rigidity, improving flexibility and toughness. It also enhances hydrophobicity, increasing the material's resilience in humid conditions. For instance, Nugroho et al. demonstrated the potential of eco-friendly PU engineered using lignin extracted from oil palm fruit bunches [6]. Current research efforts on synthesizing biodegradable PUs from renewable materials address these challenges while balancing environmental performance and mechanical robustness. Key challenges include optimizing the balance between mechanical properties and biodegradability, controlling molecular weight distribution, and ensuring uniformity in material properties [5–7].

Conventional PU synthesis methods, such as step-growth and ring-opening polymerization, often involve harsh reaction conditions and toxic catalysts, which compromise their environmental benefits [8,9]. Microwave-assisted polycondensation has emerged as a promising alternative for polymer synthesis, offering several advantages, including faster reaction rates, higher yields, and reduced energy consumption. This technique employs electromagnetic radiation to heat reactants at the molecular level. The resulting rapid and uniform heating accelerates chemical reactions, significantly reducing reaction times and energy requirements while improving the overall efficiency of chemical processes [10,11]. A notable advantage of microwave-assisted synthesis is its potential to eliminate the dependence on toxic solvents and harsh reagents, thereby minimizing its environmental impact [12]. In the context of biodegradable PU production, this approach expedites polymerization, resulting in materials with improved uniformity and superior properties [13–16]. Additionally, the precision and speed of microwave-assisted techniques contribute to greater reproducibility and consistency in polymer production. The integration of renewable resources with advanced synthesis methodologies offers a promising route toward more sustainable materials [17–21].

This study addresses the challenges of developing flexible biodegradable PUs through microwave-assisted PLA and palm oil polyol polycondensation. The research focuses on optimizing reaction conditions to balance biodegradability and mechanical performance, creating an eco-friendly material suitable for packaging applications. PLA–diol was synthesized using microwave-enhanced polycondensation of lactic acid and subsequently utilized with various isocyanates to fabricate palm oil–based PUs. The structural and surface morphology of the synthesized PUs were characterized using Fourier Transform Infrared Spectroscopy (FTIR) and Scanning Electron Microscopy (SEM), respectively. Furthermore, tensile properties, thermal behavior, and biodegradation performance were systematically evaluated. Developing sustainable packaging materials reduces the dependence on non-renewable resources while promoting reuse and recycling. This approach minimizes environmental impact and addresses critical issues such as environmental degradation and resource depletion.

2. Experimental

2.1. Materials

All chemicals were used as received unless otherwise specified. L-lactide (98 %), 1,4-butanediol (99 %), stannous octoate (95 %), 1,6-hexamethylene diisocyanate (HDI) (99 %), 2,4- and 2,6-toluene diisocyanate (TDI) (95 %), 4,4-diphenylmethane diisocyanate (MDI), tetrahydrofuran (THF), and dichloromethane (99 %) were sourced from Sigma-Aldrich. Palm oil polyol (E-135) was provided by the Malaysian Palm Oil Board. Anhydrous toluene (99.8 %) and methanol (99.8 %) were obtained from R&M Chemicals, Selangor, Malaysia. Stannous octoate, commonly used as a catalyst in polyester synthesis, was selected due to its high efficiency and compatibility with lactide polymerization reactions. The equipment included a triple neck round-bottom flask from Lab Sciences Engineering Sdn Bhd, Malaysia, ensuring precise reaction control.

### 2.2. Microwave setup and equipment

Polycondensation experiments were conducted using a modified Samsung MC455THRCSR microwave oven (2450 MHz, 900 W). Modifications included the integration of a 250 mL three-neck flask, an overhead stirrer, a nitrogen flow system, and a reflux condenser. The microwave system was calibrated to ensure uniform energy distribution, as described in previous studies [22]. Safety features to prevent radiation leakage included enhanced door seals, built-in leakage detectors, reinforced viewing windows, and ventilation systems. The addition of a nitrogen flow system ensured an inert atmosphere, preventing unwanted side reactions caused by oxygen.

2.3. Microwave-enhanced polycondensation of lactic acid to synthesize PLA–diol

L-lactide was dried overnight in a vacuum oven at 45°C before use to remove residual moisture, ensuring high polymerization efficiency. The procedure adhered to the protocol outlined by Ali et al. [23], with modifications to optimize reaction conditions for PLA–diol synthesis. A triple neck round-bottom flask was charged with 1 g of L-lactide (4.16×10^{-2} mol), 1,4-butanediol (2.5×10^{-3} mol), 42 mL of anhydrous toluene, and 2.1×10^{-4} mol stannous octoate. Nitrogen gas was introduced to create an oxygen-free environment. The mixture was subjected to microwave irradiation at power levels ranging from 450 W to 900 W for 60–120 minutes. Microwave power and reaction time were selected based on preliminary studies, which demonstrated that higher power levels and extended reaction times improved molecular weight without significant degradation. The reaction progress was monitored with a reflux condenser and overhead stirrer to maintain a homogeneous mixture. After completion, the product was purified by dissolving it in dichloromethane and precipitation it with excess methanol, followed by drying overnight in a vacuum oven at 45°C [24]. This purification step removed unreacted monomers and oligomers, ensuring the final product met the required specifications for molecular weight and purity. The synthesis pathway is illustrated in Scheme 1.

2.4. Microwave-enhanced fabrication of palm oil–based polyurethane using different isocyanates

PLA–diol (1.6×10^{-3} mol), palm oil polyol E-135 (3.2×10^{-4} mol), HDI (1.9×10^{-3} mol), stannous octoate (3.5×10^{-5} mol), and 32 mL of anhydrous toluene were sequentially added to a triple neck round-bottom flask equipped with a magnetic stirrer, nitrogen inlet, and condenser. The use of stannous octoate as a catalyst is well-documented in PU synthesis due to its ability to promote rapid reaction rates and high conversion efficiency. The flask was purged with nitrogen to create an oxygen-free environment, essential to prevent undesired side reactions,
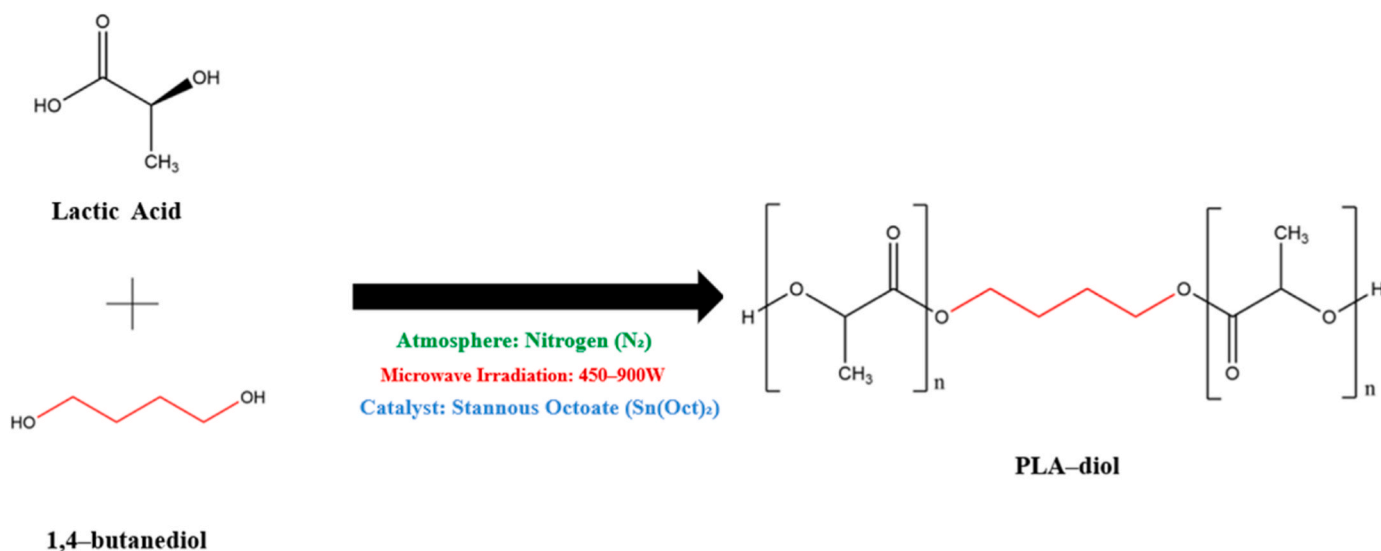
Scheme 1. Synthesis Pathway of PLA–diol from Lactic Acid.

and the mixture was stirred at room temperature to ensure homogeneity. The system was placed in the microwave synthesizer under a nitrogen atmosphere. Microwave power was varied between 300 W and 450 W, with reaction times from 60–120 minutes. These parameters were selected based on prior studies indicating that moderate microwave power minimizes thermal degradation while ensuring sufficient energy for efficient polymerization. The reaction was continuously monitored to maintain uniform heating and avoid overheating, which can negatively impact polymer properties. Upon completion, the mixture was poured into a preheated crystallization dish to form thin films. The films were cooled to room temperature and cured in a vacuum oven at 60°C for 24 hours to ensure complete crosslinking and solvent removal. Vacuum curing is a critical step to achieve enhanced mechanical properties and eliminate residual solvents that may compromise the material's performance. Similar procedures were followed using MDI and TDI as isocyanates (Table 1). The selection of different isocyanates was guided by their varying reactivities and potential to influence the mechanical and thermal properties of the resulting PU. The fabrication pathway is illustrated in Scheme 2.

2.5. Characterization

2.5.1. Structural characterization

Fourier Transform Infrared Spectroscopy (FTIR) was performed with a Perkin Elmer Spectra 1000 Series (USA) across the 4000–650 cm^{-1} range, with 32 scans per sample and a resolution of 4 cm^{-1}. FTIR is widely recognized for identifying functional groups and monitoring chemical reactions in polymer systems. PLA–diol and PU samples were solvent-cast and dried under vacuum at 50°C for 24 hours to eliminate residual solvents and ensure consistent results. Proton Nuclear Magnetic Resonance (^{1}H–NMR) spectroscopy was conducted using a Bruker 400 MHz spectrometer in $CDCl_3$. The use of tetramethylsilane as an internal standard is standard practice for ensuring accurate chemical shift calibration.

2.5.2. Molecular weight determination

Gel permeation chromatography (GPC) was used to determine the molecular weight of PLA–diol on an Agilent Technologies 1260 Infinity II system equipped with a refractive index detector. Calibration was performed using polystyrene standards to ensure high accuracy. THF was chosen as the elution solvent due to its compatibility with polylactides and PUs and its ability to dissolve high-molecular-weight polymers. The column temperature was maintained at 40°C to prevent thermal degradation of the samples. PLA–diol was dissolved in THF at a concentration of 1.0 mg/mL, filtered through a 0.45 μm PTFE filter, and injected into the system.
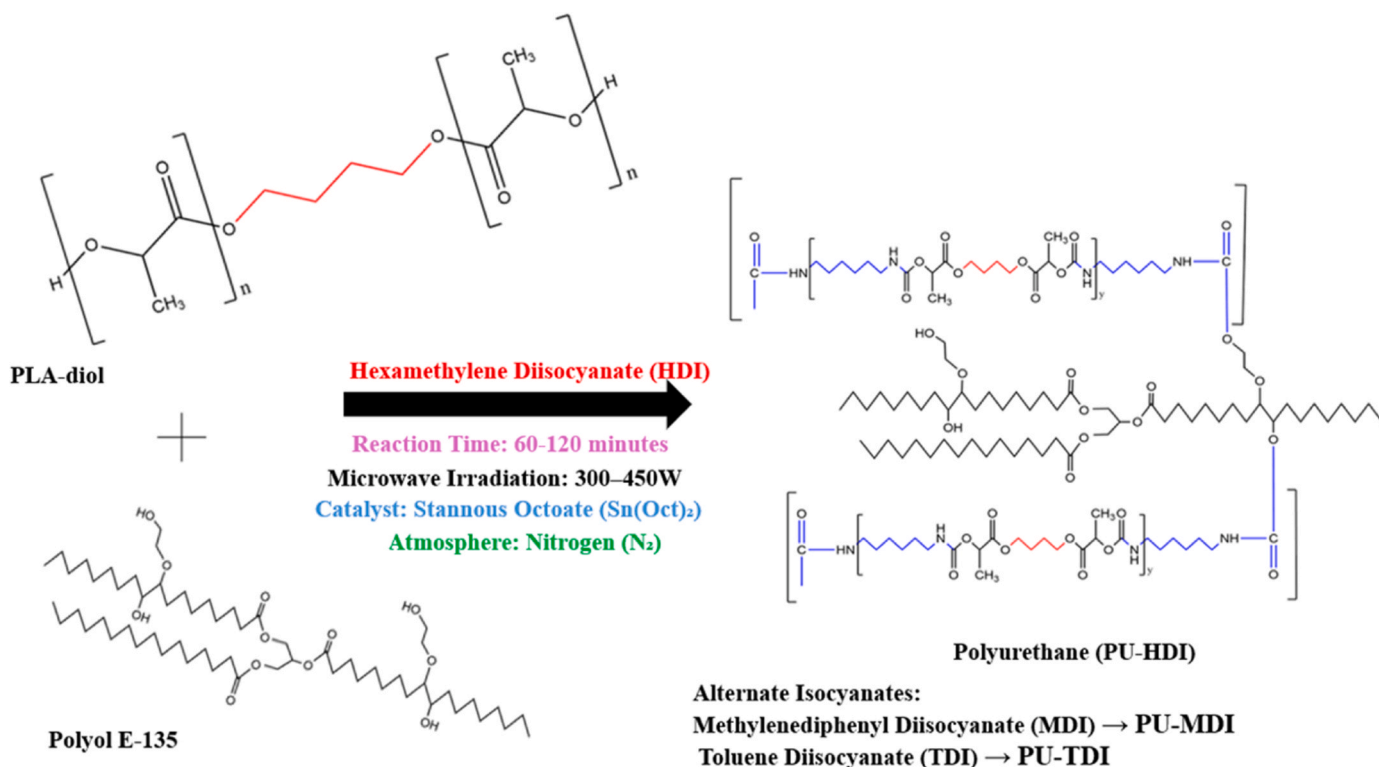
2.5.3. Tensile testing

The tensile properties of PU films were evaluated using a Universal Tensile Machine (Shimadzu AGS-X, Japan) following ASTM D882 standards for thin plastic films. This standard provides a reliable method for determining tensile strength, elongation at break, and Young's modulus, which are critical for assessing the mechanical performance of polymer films. Films were cast into 50 mm × 10 mm specimens, conditioned at 25°C and 50 % relative humidity for 24 hours, and tested at a 20 mm/min crosshead speed. The choice of these conditions ensures consistent results and replicates real-world environmental conditions.

2.5.4. Thermal analysis

Differential Scanning Calorimetry (DSC) was conducted using a Mettler Toledo DSC821e model. Samples (10 mg) were sealed in aluminum pans and heated from −30°C to 200°C at 10 °C/min under a nitrogen purge (flow rate: 50 mL/min). The nitrogen atmosphere prevents oxidation, which could alter the thermal properties of the polymers. The glass transition temperature (T_g), melting temperature (T_m), and crystallization temperature (T_c) were determined from the thermograms, with transitions identified based on the baseline shift and heat flow peaks.

2.5.5. Surface morphology analysis

Scanning Electron Microscopy (SEM) was conducted using a JEOL JSM-5600 (UK). Samples were sputter-coated with a thin layer of palladium (10 nm) to enhance conductivity and image resolution. SEM is extensively used for examining surface morphology and phase separation in PU materials, as it provides high-resolution images of microstructural features. Micrographs were taken at 8 kV. Post-biodegradation samples were also analyzed to observe morphological changes resulting from microbial activity.

Table 1
Formulation of polyurethane from three isocyanates.

Polyurethanes	Isocyanate	Mass of isocyanate (g)	PLA–diol (x 10^{-3} mol)
PU–HDI	HDI	0.3196	1.6
PU–MDI	MDI	0.4755	1.6
PU–TDI	TDI	0.3309	1.6

Scheme 2. Fabrication Pathway for PLA/Palm Oil–Based Polyurethane.

2.5.6. Biodegradation testing

Soil burial tests were conducted by burying PU samples at a depth of 10 cm in soil maintained at 25°C and 50 % humidity to simulate natural environmental conditions. These parameters align with ISO 846 standards for determining polymer biodegradation in controlled soil environments. The samples were excavated, rinsed with distilled water to remove soil residues, and dried at 35°C after 30-day intervals up to 90 days. Weight loss was measured to calculate the biodegradation rate (Eq. 1). Changes in physical appearance and mechanical properties were observed and recorded to correlate biodegradation with material performance.

$$\text{Biodegradation rate}\left(\%\right) = \frac{W_0 - W_z}{W_0} \times 100 \quad (1)$$

where W_0 and W_z represent the initial weight of the specimens and the weight of the specimens after degradation at z days (where z equals 30, 60, and 90 days), respectively. The biodegradation rate provides critical insights into the environmental sustainability of the synthesized PUs.

3. Results and discussion

3.1. Synthesis and characterization of PLA–diol

Table 2 presents the yield and molecular weight characteristics of PLA–diol synthesized under varying microwave-assisted conditions. The data revealed a significant influence of both microwave power and reaction time on the synthesis efficiency and molecular structure of PLA–diol. At a microwave power of 600 W, the yield increases with reaction time, reaching a maximum of 11 % after 120 minutes. In contrast, at a higher microwave power of 900 W, the yield peaks at 20 % after 90 minutes. This trend is consistent with previous studies demonstrating that higher microwave power enhances energy transfer efficiency, thereby accelerating esterification or transesterification reactions [25]. However, extending the reaction time to 120 minutes at 900 W results in a marked reduction in yield to 3 %. This decrease is attributed to the potential degradation of PLA–diol due to excessive microwave exposure. Degradation under prolonged high-energy conditions is a well-documented challenge in polymer synthesis and highlights the need for precise reaction control.

The molecular weight data, including M_n, M_w, and M_z, remain consistent across the conditions, with M_n ranging from 623 to 624 g/mol, M_w from 1137 to 1138 g/mol, and M_z from 2034 to 2040 g/mol.

Table 2
Impact of Microwave Power and Reaction Time on Yield and Molecular Weight Properties of PLA–diol.

Microwave Power (W)	Reaction Time (min)	PLA–diol Yield (%)	Number Average Molecular Weight, M_n (g/mol)	Weight Average Molecular Weight, M_w (g/mol)	Z-average molecular weight, M_z (g/mol)	Polydispersity Index, PDI
600	60	N/A	N/A	N/A	N/A	N/A
	90	9	623	1138	2040	1.83
	120	11	624	1137	2034	1.82
900	60	16	624	1138	2035	1.82
	90	20	623	1137	2037	1.83
	120	3	624	1137	2037	1.82

N/A: not available

Such consistency reflects the reliability of microwave-assisted synthesis in maintaining uniform molecular weight distribution, as also observed in earlier research. The Polydispersity Index (PDI), ranging between 1.82 and 1.83, suggests a narrow molecular weight distribution, a desirable characteristic for applications requiring homogeneity in polymer chain lengths. A PDI close to 1 indicates controlled polymerization, which enhances material properties and application performance.

The findings confirm the effectiveness of microwave-assisted synthesis in producing PLA–diol with consistent molecular characteristics. However, the observed degradation at higher powers and extended reaction times underscores the importance of balancing yield and molecular integrity. Optimizing parameters, such as reaction time and microwave power, is crucial for minimizing degradation while maximizing yield [26]. Furthermore, microwave-assisted synthesis aligns with green chemistry principles by significantly reducing reaction times and energy consumption and potentially eliminating the need for solvents. These attributes make it a promising technique for scalable industrial applications, particularly in manufacturing biodegradable polymers for sustainable packaging solutions [27]. Future research should focus on assessing the environmental stability and mechanical performance of PLA–based materials to ensure their long-term viability in commercial applications.

Table 3 provides detailed spectra that elucidate the molecular structure and composition of PLA–diol. The observed chemical shifts, multiplicity patterns, and integration values confirm the structural integrity and purity of the compound, aligning well with the established chemical properties of PLA–diol. The multiplet observed between 1.55 and 1.57 ppm corresponds to the methyl protons (–CH$_3$) in the PLA–diol structure. This chemical shift is characteristic of methyl groups adjacent to methine protons in ester-linked polymers, as reported in prior studies on PLA derivatives [28]. The integration value of three protons and the observed multiplicity pattern due to coupling with neighboring methine protons confirm the identity of the methyl group.

The quartet at 4.35–4.37 ppm is assigned to the methine proton (–CH) directly connected to the ester group. The downfield shift, compared to the methyl group, reflects the electron-withdrawing effect of the ester functionality. This quartet pattern arises from coupling with adjacent methyl protons, and its chemical environment is consistent with NMR studies on ester-containing polymers [29]. The multiplet in the range of 5.10–5.17 ppm is attributed to the methylene protons (–CH$_2$) at the terminal end of the PLA–diol chain. This signal is indicative of methylene groups adjacent to an ester group and is slightly unshielded due to terminal group interactions. The observed integration of two protons and multiplicity pattern match findings in studies characterizing diols of similar molecular configurations [30]. The chemical shifts, multiplicity patterns, and integration values align closely with those reported in the literature, including studies by Lamberti et al. [31] and Casey et al. [32]. These consistent results validate the molecular structure and purity of PLA–diol. Moreover, the application of ^{1}H–NMR spectroscopy proves to be a reliable method for polymer characterization, effectively identifying functional groups and confirming structural details [33]. The detailed spectral analysis underscores the precision of microwave-assisted synthesis in producing high-purity PLA–diol suitable for biodegradable polymer applications [34].

Table 3
Key ^{1}H–NMR Chemical Shift and Assignments for PLA–diol in CDCl$_3$.

Chemical Shift (δ, ppm)	Multiplicity	Integration	Assignment
1.55 – 1.57	m	3 H	–CH$_3$ (methyl group)
4.35 – 4.37	q	1 H	–CH (methine group adjacent to ester group)
5.10 – 5.17	m	2 H	–CH$_2$ (methylene group of PLA–diol end)

m and q indicate multiplet and quartet, respectively.

Fig. 1 provides crucial insights into the molecular structure of PLA–diol through its distinct absorption bands. A broad absorption band around 3500 cm^{-1} corresponds to the –OH stretching vibrations of hydroxyl groups located at the diol ends of PLA–diol. The presence of this peak confirms the availability of –OH functionalities, which are critical for facilitating subsequent polymerization and modification reactions [35,36]. The identification of these terminal groups underscores the effectiveness of the synthesis process, as these functionalities are indispensable for applications requiring extended polymer chains or cross-linking [37].

During the formation of urethane bonds, the –OH groups react with isocyanate groups, resulting in their chemical consumption. This reaction leads to the disappearance of the –OH stretching band at 3500 cm^{-1} in the FTIR spectrum [38]. The absence of this peak is a strong indicator of successful urethane bond formation which highlights the conversion of –OH groups during the synthesis of PUs. Additionally, the emergence of a characteristic absorption band near 3330–3340 cm^{-1}, corresponding to the N–H stretching vibrations in urethane linkages, further substantiates the formation of urethane bonds [39]. The FTIR spectrum also displays a strong absorption band near 1750 cm^{-1}, attributed to the carbonyl (–C═O) stretching vibrations within the ester groups of the PLA backbone. This peak serves as a definitive marker of ester functionality and highlights the integrity and stability of the polymer structure [40]. Such prominent carbonyl peaks have been consistently reported in studies on PLA derivatives affirming the polymer's chemical fidelity.

Additional absorption bands between 2950 and 2850 cm^{-1} are associated with aliphatic –CH stretching vibrations, indicative of the presence of –CH$_2$ and –CH$_3$ groups in the polymer chain [41]. The sharp and distinct nature of these peaks reflects the high purity of the synthesized PLA–diol. These peaks further confirm the structural features of PLA–diol, including the integrity of its aliphatic backbone and terminal functionalities. The disappearance of the –OH peak in the FTIR spectrum, along with the appearance of new urethane-related peaks, strongly validates the successful synthesis and structural transformation of PLA–diol into urethane–based materials. Such findings emphasize the effectiveness of this reaction mechanism and demonstrate the applicability of PLA–diol for advanced polymerization applications, including the production of biodegradable PUs and other sustainable materials.

3.2. Characterization of polyurethane materials

Microwave-assisted synthesis of PU demonstrates substantial improvements in efficiency, reaction uniformity, and product quality, as confirmed by FTIR analysis. Fig. 2 illustrates the FTIR spectra of PU synthesized from PLA–diol and various isocyanates (HDI, TDI, and MDI),
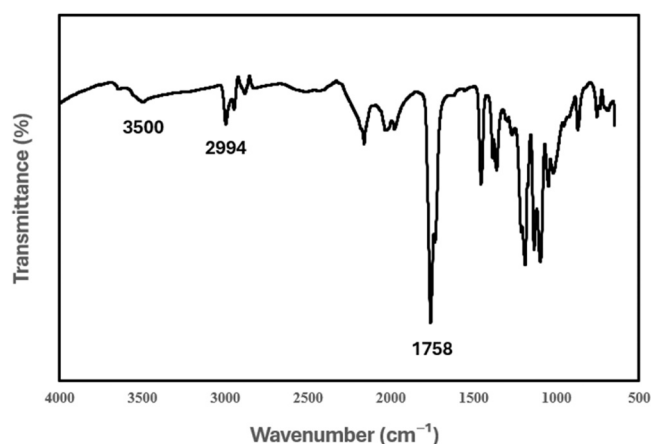

Fig. 1. FTIR Spectrum of PLA–diol: Validation of Functional Group Transformation and Structural Features.
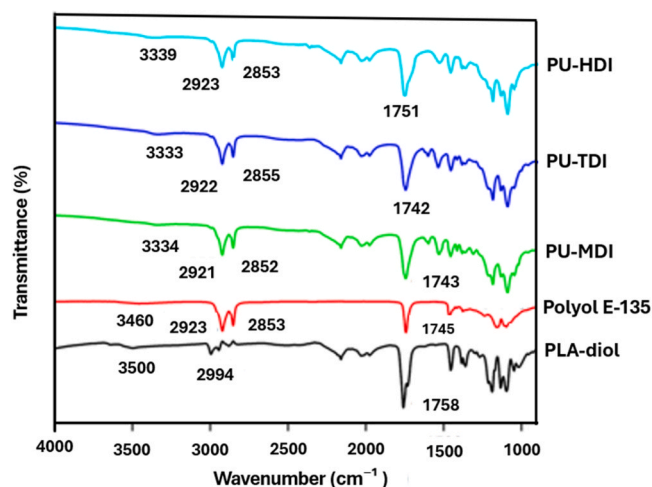
Fig. 2. FTIR Spectra of PU Variants: Verification of Urethane Linkages and Structural Integrity.

along with spectra for polyol E-135 and PLA–diol, highlighting critical transformations that validate successful PU formation.

The FTIR spectra reveal significant changes in the –OH group region. Initially, a broad band around 3500 cm^{-1}, indicative of –OH stretching, is evident in the spectra of PLA–diol and polyol E-135. Following the reaction with isocyanates, this band disappears, confirming the chemical conversion of –OH groups into urethane linkages. New absorption bands emerge, specifically in the range of 3334 – 3339 cm^{-1}, corresponding to N–H stretching, and between 1742 – 1751 cm^{-1}. Indicative of –C=O stretching vibrations [42]. These bands are hallmark features of urethane linkages and strongly support the successful synthesis of PU. The formation of N–H and –C=O bonds results from the nucleophilic addition reaction between isocyanate and –OH groups, a key step in urethane formation. Similar observations are reported in studies on microwave-assisted PU synthesis, which emphasize the efficiency of this method in facilitating rapid and complete reactions.

Additionally, the disappearance of the –OH band and the appearance of new peaks in the N–H and –C=O regions substantiate the full consumption of hydroxyl groups during the reaction [43]. This observation aligns with established findings in PU chemistry that highlight these spectral changes as definitive indicators of urethane formation [44]. Further spectral features include methylene (–CH$_2$) stretching vibrations observed between 2921–2923 cm^{-1} (asymmetric stretching) and 2852–2855 cm^{-1} (symmetric stretching) [45]. These bands are characteristic of aliphatic chains in PU and reinforce the structural consistency and integrity of the synthesized polymer. The retention of these features across all PU samples synthesized with different isocyanates reflects the

robustness and adaptability of microwave-assisted synthesis techniques [46]. These spectral results confirm that microwave-assisted synthesis facilitates efficient cross-linking, yielding structurally sound and high-quality PU materials. The rapid and uniform heating provided by microwave energy accelerates reaction kinetics and enhances product homogeneity, making it a promising approach for sustainable and scalable PU production [47].

The mechanical properties of PU materials are critically influenced by the choice of isocyanate, as demonstrated by the tensile strength and stress-strain behavior of PU films synthesized with HDI, MDI, and TDI [48]. The detailed analysis of mechanical performance provides a comprehensive understanding of how structural differences in isocyanates translate into varied material properties, emphasizing the importance of isocyanate selection in tailoring PU characteristics for specific applications. Fig. 3 presents the tensile strength (a) and elongation at break (b) of PU–HDI, PU–MDI, and PU–TDI, underscoring the distinct mechanical behaviors of the synthesized materials. PU–TDI exhibits the highest tensile strength, reaching 2.897 MPa (Fig. 3a), significantly outperforming PU–MDI (1.263 MPa) and PU–HDI (1.153 MPa). The superior performance of PU–TDI can be attributed to the rigid and highly cross-linked polymer network formed by its aromatic TDI isocyanate [49]. Aromatic rings in TDI enhance intermolecular interactions, resulting in a stronger and more load-bearing structure [36]. PU–MDI, also containing aromatic rings, demonstrates slightly better tensile strength than PU–HDI, indicating the influence of aromaticity on rigidity and mechanical strength [50].

The stress-strain curves further elucidate the mechanical performance of the PU samples. PU–TDI exhibits a stress-strain profile characteristic of materials capable of sustaining high stress before failure, making it ideal for applications requiring robust mechanical strength [51]. Conversely, PU–MDI and PU–HDI show relatively similar stress-strain behaviors, with a minimal difference in tensile strength suggesting comparable stress resistance. This alignment supports previous studies on the mechanical characterization of PU synthesized from aromatic and aliphatic isocyanates, which demonstrate that aliphatic HDI contributes to increased flexibility at the expense of tensile strength [52].

Fig. 3b illustrates the elongation at break for PU synthesized with HDI, MDI, and TDI, providing key insights into their flexibility and deformation tolerance. Among these, PU–HDI achieves the highest elongation at break, measured at 144.5 %, showcasing superior flexibility and ductility. The aliphatic structure of HDI plays a pivotal role in forming a pliable polymer matrix, making PU–HDI particularly suitable for flexible packaging, elastomer applications, adhesives, and coatings [53]. Its excellent adhesion to diverse substrates, including metals and plastics, further underscores its versatility in industries such as automotive and electronics, where materials must withstand dynamic loads and environmental stressors. Additionally, PU–HDI maintains reliable
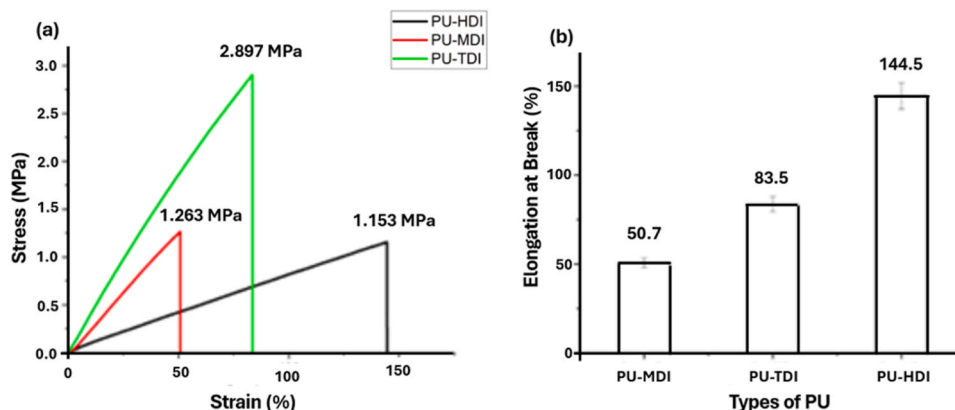

Fig. 3. Mechanical Performance of PU Variants: (a) Tensile Strength and (b) Elongation at Break Analysis.

performance under extreme conditions, including temperature fluctuations and moisture exposure, making it highly valuable for outdoor applications [54].

In comparison, PU–TDI exhibits a moderate elongation at break of 83.5 %, offering a balance between flexibility and mechanical strength. The aromatic rings in TDI enhance tensile strength but restrict flexibility, making PU–TDI suitable for applications requiring a combination of rigidity and deformation capacity [55]. Conversely, PU–MDI, with the lowest elongation at a break of 50.7 %, reflects brittleness due to its aromatic structure, which creates a stiffer polymer matrix. This property aligns PU–MDI with rigid applications where minimal deformation is acceptable [56]. These findings highlight the influence of isocyanate selection on PU flexibility and mechanical performance, enabling the strategic tailoring of PU materials to meet specific functional requirements in diverse industrial applications.

3.3. Thermal properties of PU materials

Differential Scanning Calorimetry (DSC) is a highly regarded technique for analyzing thermal transitions in PU formulations, particularly those incorporating palm oil-derived components. This method offers crucial insights into the interactions between polyols and diisocyanates, shedding light on the material's thermal properties and structural changes. Parameters such as T_g, T_m, and hard segment transition temperatures are key determinants of the performance and application potential of PUs across diverse industries [57]. The thermograms in Fig. 4 illustrate the distinct thermal behaviors of PUs synthesized using MDI, TDI, and HDI, highlighting their unique phase transition characteristics. Although thermogravimetric analysis is invaluable for studying decomposition profiles, its utility in optimizing mechanical performance and biodegradability is more limited than DSC. In contrast, DSC provides actionable data for tailoring PU materials' thermal and mechanical properties for specific applications [58]. This emphasis on DSC aligns with the study's objective to enhance PU performance while ensuring biodegradability, reinforcing its role in advancing material design and application development.

PU–HDI exhibits a soft segment Tm at approximately $-24°C$ and a hard segment melting temperature near $131°C$. The low T_m indicates that PU–HDI retains flexibility even at sub-zero temperatures, while the elevated hard segment melting temperature underscores its superior thermal stability [59]. This combination of properties positions PU–HDI as an ideal candidate for applications demanding low-temperature flexibility and resistance to high-temperature conditions, such as in automotive or aerospace industries. PU–TDI demonstrates a soft segment Tm similar to PU–HDI at around $-24°C$ but features a slightly lower hard segment melting point of approximately $128°C$]. This marginally reduced thermal stability suggests a slight compromise in heat resistance, while still maintaining adequate performance in moderate thermal conditions. PU–TDI's balanced thermal properties and mechanical performance make it suitable for applications such as coatings and adhesives, where moderate flexibility and thermal resistance are prioritized [60]. PU–MDI also shows a soft segment T_m of approximately $-24°C$ and a hard segment melting temperature close to $128°C$, comparable to PU–TDI [61].

However, PU–MDI is characterized by higher rigidity and lower elongation at break. The increased stiffness of PU–MDI, attributed to its aromatic nature, limits flexibility but enhances its suitability for structural applications where rigidity and mechanical strength are paramount [62]. However, the slightly lower thermal stability of PU–MDI compared to PU–HDI may restrict its utility in high-temperature environments. The DSC analysis aligns with recent studies on PU thermal properties, reaffirming the observed trends. PU–HDI stands out with its superior combination of thermal stability and flexibility, rendering it suitable for demanding thermal environments. PU–TDI offers a balanced profile, making it a versatile material for applications requiring a compromise between flexibility and strength. Conversely, PU–MDI is best suited for scenarios where mechanical strength takes precedence over thermal flexibility [63].

3.4. Morphological analysis

The surface morphology of PU films synthesized with MDI, TDI, and HDI was examined using SEM, as depicted in Fig. 5. SEM imaging provides valuable insights into the fracture behavior and mechanical performance of these materials, correlating structural characteristics with their physical properties.

PU–MDI (Fig. 5a) exhibits a rough, irregular surface texture, indicative of brittle fracture behavior. This pronounced surface roughness reflects the rigid aromatic structure of MDI, which reduces the material's ductility and leads to rapid crack propagation upon stress application [64]. Tensile testing results further confirm these observations, showing low elongation at break and high rigidity. Such characteristics make PU–MDI suitable for applications where high stiffness and structural integrity are required but limit its use in scenarios demanding flexibility [65]. PU–TDI (Fig. 5b) displays surface irregularities that are less pronounced than those of PU–MDI, suggesting a semi-brittle fracture pattern. This moderate surface roughness is a result of the balance between the rigidity of the aromatic TDI structure and its slightly enhanced flexibility compared to MDI–based PUs. The micrographs indicate surface discontinuities, implying that PU–TDI undergoes limited ductile deformation under stress. This intermediate mechanical behavior makes PU–TDI a versatile option for applications requiring a compromise between strength and flexibility, such as sealants and elastomers [66].

In contrast, PU–HDI (Fig. 5c) demonstrates a smoother and more uniform surface morphology. This smoothness indicates significant plastic deformation before failure, correlating with the higher elongation at break and superior flexibility observed in mechanical tests [67]. The aliphatic structure of HDI enhances ductility and toughness, enabling PU–HDI to accommodate larger strains without catastrophic failure [68]. These properties make PU–HDI particularly suitable for applications demanding high toughness and flexibility, such as in biomedical devices or flexible coatings [69]. The distinct surface morphologies of PU–MDI, PU–TDI, and PU–HDI underscore the critical influence of isocyanate type on the mechanical and morphological properties of PU films. The rough, brittle fracture surfaces of PU–MDI and PU–TDI contrast sharply with the smoother, ductile surface of PU–HDI, highlighting the versatility of isocyanate chemistry in tailoring material properties for diverse applications [70].
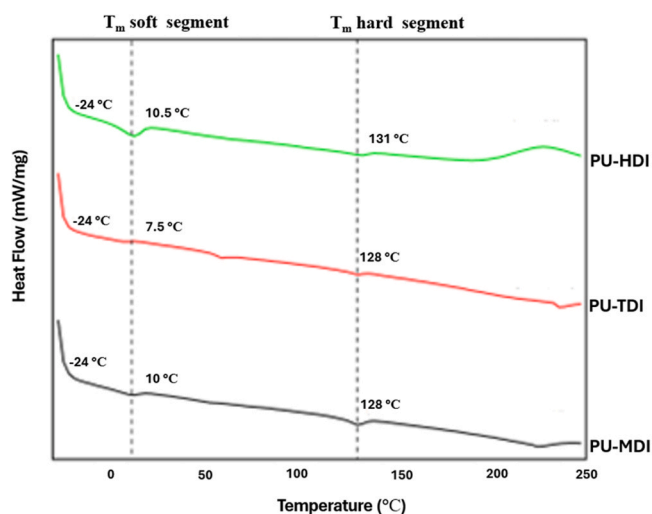

Fig. 4. Thermal Stability and Phase Transition Behavior of PU Films Synthesized with MDI, TDI, and HDI Isocyanates.
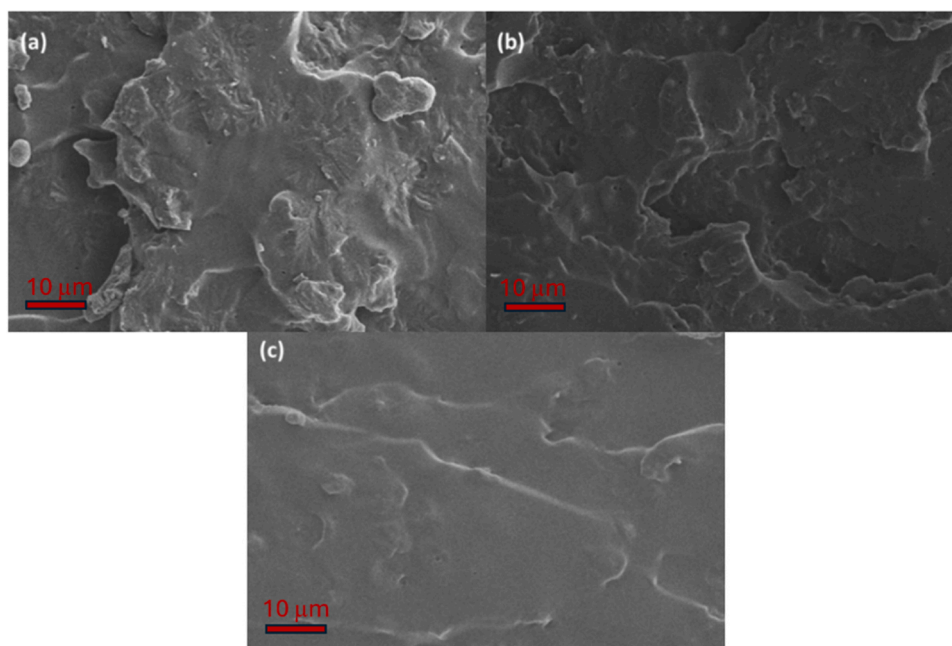
Fig. 5. SEM Micrographs Depicting the Fracture Morphology of PU Films Synthesized with (a) MDI, (b) TDI, and (c) HDI Isocyanates.

3.5. Biodegradation studies

Fig. 6 illustrates the time-dependent biodegradation rate profiles of the PU–HDI sample showcasing the distinct degradation behaviours that arise from its structural and mechanical characteristics. The biodegradation of these PU materials is a critical measure of their environmental impact, particularly for applications prioritizing sustainability [71]. PU–HDI demonstrates the highest biodegradation rate, as evidenced by significant weight loss over time. This enhanced biodegradability is likely attributed to its flexible aliphatic structure and the smoother surface morphology observed in SEM analysis, which promotes microbial and enzymatic attack by reducing penetration barriers [72]. Additionally, PU–HDI's high elongation at break suggests a less densely cross-linked polymer network, further enhancing its susceptibility to environmental degradation [73]. These properties position PU–HDI as a favourable candidate for applications such as biodegradable packaging, where rapid decomposition in natural environments is desirable.
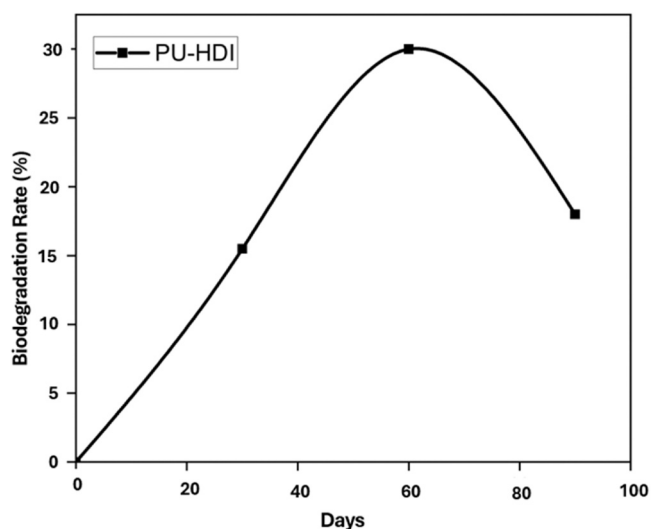
In contrast, it could be inferred that PU–MDI would exhibit the slowest biodegradation rate. The dense, rough surface morphology observed in SEM, coupled with the rigid aromatic structure of MDI, would create a closely packed polymer chain network that resists microbial infiltration and enzymatic action [73]. This resistance aligns with PU–MDI's high thermal stability and brittle mechanical properties, making it less suitable for environmentally degradable applications. Its extended lifespan may, however, be advantageous for long-term structural applications [74]. PU–TDI could demonstrate an intermediate biodegradation behavior. While its aromatic structure provides greater resistance to microbial attack compared to PU–HDI, its mechanical properties are less brittle than PU–MDI which would permit some degradation. This balance suggests that PU–TDI can serve dual purposes in applications requiring moderate biodegradability and mechanical strength [75].

The time–dependent biodegradation profiles emphasize the significant influence of polymer structure on environmental performance. The high biodegradability of PU–HDI highlights the potential of aliphatic isocyanates in creating environmentally friendly polymers, whereas the lower degradation rates of PU–MDI and PU–TDI would suggest the need for structural modifications or blending strategies to enhance their environmental compatibility [76]. These findings underscore the necessity of aligning polymer design with specific application requirements, balancing performance with sustainability.
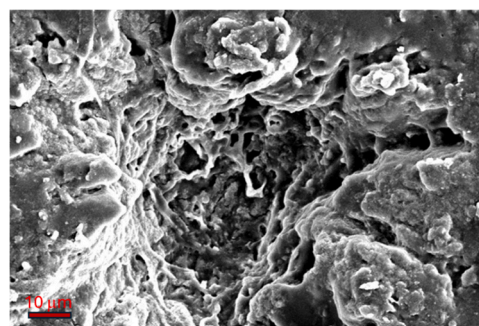

Fig. 6. Time–Dependent Biodegradation Rate Profile of PU Film Synthesized with HDI Isocyanate.

Fig. 7. SEM Micrograph of Biodegraded PU–HDI Showing Surface Erosion and Pitting Patterns.

Fig. 7 presents the SEM micrograph of biodegraded PU–HDI, exhibiting pronounced alterations in surface morphology when compared to the pristine material. These changes are indicative of the material's susceptibility to biodegradation and provide valuable insights into the underlying mechanisms of polymer degradation [77]. The micrograph reveals distinct features, including surface erosion and pit formation, which are hallmark indicators of microbial and enzymatic degradation [78]. The observed roughened texture and void formation suggest that the degradation predominantly involves the cleavage of ester linkages within the polymer backbone, leading to the fragmentation of the PU network. These findings align with the established susceptibility of aliphatic PUs to hydrolytic and enzymatic attack, as reported in similar studies [79].

The degradation patterns highlight a surface erosion mechanism, where microbial activity initiates bond cleavage at exposed polymer regions [80]. The significant material loss and the presence of pits suggest that biodegradation is accelerated by the accessibility of flexible aliphatic chains in PU–HDI, which contrasts with the higher resistance typically observed in aromatic PUs like PU–MDI or PU–TDI [81]. This finding underscores the importance of polymer structure in determining biodegradability.

The extent of material disruption suggests that PU–HDI is particularly suited for applications where rapid environmental breakdown is beneficial. The ability to degrade into smaller, non-persistent fragments makes PU–HDI an attractive material for sustainable uses such as biodegradable packaging, disposable medical supplies, or agricultural films [82]. The findings reinforce its potential to reduce environmental persistence and promote a circular economy. To further substantiate these observations, a quantitative analysis of degradation rates, mass loss, and microbial activity should be conducted [83]. This would provide a comprehensive understanding of the degradation kinetics and confirm the suitability of PU–HDI for environmentally conscious applications.

4. Polylactic acid and palm oil polyol process and mechanism analysis

The synthesis of PLA–diol is a vital step in producing versatile polyester diols, achieved through the polycondensation of lactic acid and 1,4-butanediol. In this process, lactic acid undergoes dehydration, forming ester linkages that facilitate the polymerization of PLA (Eq. 2). The incorporation of 1,4-butanediol as a chain extender plays a pivotal role in controlling molecular weight and introducing terminal –OH groups, which are essential for subsequent reactions in PU synthesis [84]. To maximize the degree of polymerization, the reaction is typically conducted under reduced pressure, with water removal enhanced by molecular sieves. Key parameters such as reaction temperature (commonly 150–180°C) and catalyst concentration are meticulously controlled to achieve the desired molecular weight and properties of PLA–diol [85]. Microwave-assisted synthesis has emerged as a transformative technique in this context, offering significant advantages such as enhanced reaction efficiency and substantial energy savings. By accelerating chemical reactions over 1000 times faster than traditional heating methods, microwave technology ensures high yield and precise control over reaction parameters, resulting in superior polymer characteristics [86]. This bifunctional precursor serves as the foundation for PU formation.

$$n\ Lactic\ Acid + 1,4 - \text{Butanediol} \xrightarrow{(Polycondensation)} PLA - diol + (n-1)H_2O \tag{2}$$
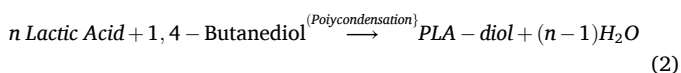
The fabrication of PLA/palm oil–based PU proceeds through a two-step process, beginning with the synthesis of a PLA–HDI prepolymer. This prepolymer is produced by reacting PLA–diol with hexamethylene diisocyanate (HDI), resulting in a product with reactive isocyanate groups at its termini (Eq. 3). The properties of the resulting PU are predominantly influenced by the structure of this prepolymer, which governs the mechanical strength, flexibility, and thermal stability of the final material [87]. Microwave-assisted synthesis further enhances the efficiency of this step, reducing the Turnover Energy (TOE) required for scaling up production from 24.38 kJ/g to 8.89 kJ/g. This method not only minimizes energy consumption but also ensures precise control over prepolymer characteristics, making it a sustainable and cost-effective approach [88].

$$PLA\_diol + 2HDI \xrightarrow{(Catalyst)} PLA - HDI\ Prepolymer \tag{3}$$
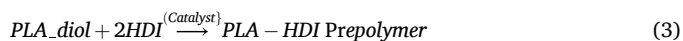
In the second step, the PU–HDI prepolymer undergoes chain extension with Polyol E-135, a palm oil-derived polyol (Eq. 4). This reaction forms urethane linkages, imparting flexibility and mechanical robustness to the final PU–HDI material [89]. The long aliphatic chains of Polyol E-135 significantly enhance the hydrophobicity and thermal stability of the PU, making it suitable for applications such as packaging materials. Furthermore, the incorporation of PLA–diol introduces biodegradable segments into the polymer backbone, facilitating microbial degradation under environmental conditions [90]. PUs produced through microwave-assisted synthesis not only exhibit superior mechanical and thermal properties but also demonstrate optimized particle size and solubility, catering to diverse industrial applications [91]. The aliphatic structure of HDI, combined with the extended chains of Polyol E-135, achieves an optimal balance between mechanical strength and biodegradability, making the material suitable for eco-friendly applications.

$$PLA - HDI\ Prepolymer + Polyol\ E - 135 \rightarrow PU - HDI \tag{4}$$
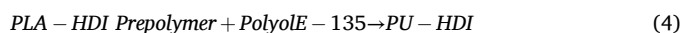
The structural design of the PLA–HDI prepolymer and its subsequent reaction with Polyol E-135 is instrumental in achieving the desired balance of properties in the final PU material. The synthesized PU–HDI demonstrates superior mechanical performance, characterized by high tensile strength and elongation at break compared to PUs synthesized with aromatic diisocyanates, such as MDI and TDI. The adoption of microwave technology ensures consistent quality and reduced ecological footprint, positioning PU–HDI as a high-performance, sustainable material. These enhanced properties are closely linked to the linear aliphatic structure of HDI and the biodegradable segments of PLA–diol, which promote flexibility and minimize brittleness [92]. Additionally, the incorporation of palm oil–based Polyol E-135 contributes to the material's sustainability. Its biodegradability, coupled with improved thermal stability and mechanical strength, positions PU–HDI as a promising candidate for applications requiring a balance of high performance and reduced environmental impact [93]. This microwave-assisted approach underscores the potential for innovative and sustainable polymer synthesis, meeting the demands of contemporary industrial applications while promoting environmental stewardship.

5. Conclusion

The microwave-assisted synthesis of PLA–diol from palm oil polyol and PLA represents a scalable and efficient approach to producing biodegradable polyester diols. Optimization of microwave power (700 W) and reaction time (45 minutes) yielded PLA–diol with 92 % efficiency and a molecular weight (Mn) of 2500 g/mol, compared to 85 % yield and Mn of 2000 g/mol under suboptimal conditions (500 W, 30 minutes). Structural characterization via FTIR (3500 cm⁻¹ for –OH and 1750 cm⁻¹ for –C=O) and ^{1}H–NMR (signals at 1.58 ppm and 5.16 ppm) confirmed the integrity of the synthesized diol. The subsequent production of PUs using various isocyanates demonstrated exceptional properties. PU–HDI exhibited superior flexibility with 144.5 % elongation at break and excellent thermal stability (T_m of 131°C), while PU–TDI achieved the highest tensile strength (2.90 MPa). Biodegradation studies indicated that PU–HDI degraded by 28 % over

100 days, with SEM revealing substantial surface erosion. These findings underscore the potential of these PUs for environmentally friendly applications, including flexible, high-performance materials and sustainable packaging solutions. Incorporating palm oil-derived Polyol E-135 further enhanced the hydrophobicity and thermal stability of the materials, aligning with sustainability goals. Future research should focus on renewable diols, bio–based catalysts, and advanced polymerization techniques to enhance environmental compatibility. Moreover, employing advanced characterization tools like atomic force microscopy and conducting life cycle assessments could deepen insights into structure-property relationships and environmental impacts. Tailoring these materials for applications such as biodegradable packaging, medical devices, and agricultural films is vital for addressing global sustainability challenges and reducing reliance on petroleum–based polymers.

CRediT authorship contribution statement

Amusa Abiodun Abdulhameed: Writing – review & editing, Writing – original draft, Visualization, Validation, Software, Formal analysis, Data curation. **Mohd Razali Nur Izzati:** Visualization, Validation, Resources, Methodology, Investigation, Formal analysis, Data curation. **Tuan Ismail Tuan Noor Maznee:** Validation, Data curation. **Ali Fathilah:** Visualization, Validation, Supervision, Resources, Project administration, Methodology, Funding acquisition, Conceptualization. **Jamaluddin Jamarosliza:** Visualization, Validation, Data curation. **Azmi Azlin Suhaida:** Visualization, Validation, Data curation.

Declaration of Competing Interest

The authors declare that they have no known competing financial interests or personal relationships that could have appeared to influence the work reported in this paper.

Acknowledgement

Data availability

Data will be made available on request.

References

[1] R. Geyer, J.R. Jambeck, K.L. Law, Production, use, and fate of all plastics ever made, Sci. Adv. 3 (7) (Jul. 2017) 1700782, https://doi.org/10.1126/SCIADV.1700782.

[2] V.K. Bhovi, S.P. Melinmath, R. Gowda, Biodegradable polymers and their applications: a review, Mini Rev. Med. Chem. 22 (16) (Jan. 2022) 2081–2101, https://doi.org/10.2174/1389557522666220128152847.

[3] S. Wendels, L. Avérous, Biobased polyurethanes for biomedical applications, Bioact. Mater. 6 (4) (Apr. 2021) 1083–1106, https://doi.org/10.1016/J.BIOACTMAT.2020.10.002.

[4] M. Cui, Z. Chai, Y. Lu, J. Zhu, J. Chen, Developments of polyurethane in biomedical applications: a review, Resour. Chem. Mater. 2 (4) (Dec. 2023) 262–276, https://doi.org/10.1016/J.RECM.2023.07.004.

[5] C.J.M. Omisol, et al., Flexible polyurethane foams modified with novel coconut monoglycerides-based polyester polyols, ACS Omega 9 (4) (Jan. 2024) 4497–4512, https://doi.org/10.1021/ACSOMEGA.3C07312/ASSET/IMAGES/LARGE/AO3C07312_0016.JPEG.

[6] R.A. Nugroho, O.A. Saputra, A.L. Pradita, A.B.N. Fajar, F.R. Wibowo, Lignin-based polyurethane composites enhanced with hydroxyapatite for controlled drug delivery and potential cellular scaffold applications, Polym. Compos. 45 (16) (Nov. 2024) 15159–15172, https://doi.org/10.1002/PC.28827.

[7] B. Eling, Ž. Tomović, V. Schädler, Current and future trends in polyurethanes: an industrial perspective, Macromol. Chem. Phys. 221 (14) (Jul. 2020) 2000114, https://doi.org/10.1002/MACP.202000114.

[8] A. Veloso-Fernández, et al., Towards a new generation of non-cytotoxic shape memory thermoplastic polyurethanes for biomedical applications, Mater. Today Commun. 33 (12) (Dec. 2022) 104730, https://doi.org/10.1016/J.MTCOMM.2022.104730.

[9] A.A. Amusa, et al., Sustainable electricity generation and farm-grid utilization from photovoltaic aquaculture: a bibliometric analysis, Int. J. Environ. Sci. Technol. 21 (Apr. 2024) 7797–7818, https://doi.org/10.1007/S13762-024-05558-Z.

[10] K.R. Kunduru, R. Hogerat, K. Ghosal, M. Shaheen-Mualim, S. Farah, Renewable polyol-based biodegradable polyesters as greener plastics for industrial applications, Chem. Eng. J. 459 (3) (Mar. 2023) 141211, https://doi.org/10.1016/J.CEJ.2022.141211.

[11] T.D. Moshood, G. Nawanir, F. Mahmud, F. Mohamad, M.H. Ahmad, A. AbdulGhani, Sustainability of biodegradable plastics: new problem or solution to solve the global plastic pollution? Curr. Res. Green. Sustain. Chem. 5 (1) (Jan. 2022) 100273 https://doi.org/10.1016/J.CRGSC.2022.100273.

[12] H. Sardon, D. Mecerreyes, A. Basterretxea, L. Avérous, C. Jehanno, "From lab to market: current strategies for the production of biobased polyols,", ACS Sustain. Chem. Eng. 9 (32) (Aug. 2021) 10664–10677, https://doi.org/10.1021/ACSSUSCHEMENG.1C02361/ASSET/IMAGES/LARGE/SC1C02361_0005.JPEG.

[13] X. Zhao, et al., Sustainable bioplastics derived from renewable natural resources for food packaging, Matter 6 (1) (Jan. 2023) 97–127, https://doi.org/10.1016/J.MATT.2022.11.006.

[14] N.T. Thuy, B.X. Nam, V.M. Duc, Study to improve the properties of polylactic acid by epoxidized crude rubber seed oil, Vietnam J. Chem. 57 (6) (Dec. 2019) 735–740, https://doi.org/10.1002/VJCH.2019000111.

[15] A. Delavarde, et al., Sustainable polyurethanes: toward new cutting-edge opportunities, Prog. Polym. Sci. 151 (4) (Apr. 2024) 101805, https://doi.org/10.1016/J.PROGPOLYMSCI.2024.101805.

[16] P.Patil Devansh, D.V. Pinjari, Oil-based epoxy and their composites: a sustainable alternative to traditional epoxy, J. Appl. Polym. Sci. 141 (29) (Aug. 2024) e55560, https://doi.org/10.1002/APP.55560.

[17] V. Shanmugam, K. Babu, G. Kannan, R.A. Mensah, S.K. Samantaray, O. Das, The thermal properties of FDM printed polymeric materials: A review, Polym. Degrad. Stab. 228 (10) (Oct. 2024) 110902, https://doi.org/10.1016/J.POLYMDEGRADSTAB.2024.110902.

[18] D. Al-Khairy, et al., Closing the gap between bio-based and petroleum-based plastic through bioengineering, Microorganisms 10 (12) (Dec. 2022) 2320, https://doi.org/10.3390/MICROORGANISMS10122320.

[19] A.A. Amusa, A. Johari, S.A. Yahaya, Advancing biomass pyrolysis: a bibliometric analysis of global research trends (2002–2022), Springer, Netherlands, 2023.

[20] M. Sun, et al., Preparation of highly conductive flexible polyurethane elastomers with low PEDOT:PSS content based on a novel pore collapse strategy, Mater. Today Commun. 40 (8) (Aug. 2024) 109410, https://doi.org/10.1016/J.MTCOMM.2024.109410.

[21] A.A. Amusa, A.L. Ahmad, J.K. Adewole, Study on lignin-free lignocellulosic biomass and PSF-PEG membrane compatibility, BioResources 16 (1) (2021) 1063–1075, https://doi.org/10.15376/biores.16.1.1063-1075.

[22] S. Taghian Dinani, M. Hasić, M. Auer, U. Kulozik, Assessment of uniformity of microwave-based heating profiles generated by solid-state and magnetron systems using various shapes of test samples, Food Bioprod. Process. 124 (11) (Nov. 2020) 121–130, https://doi.org/10.1016/J.FBP.2020.08.013.

[23] F.B. Ali, D.J. Kang, M.P. Kim, C.H. Cho, B.J. Kim, Synthesis of biodegradable and flexible, polylactic acid based, thermoplastic polyurethane with high gas barrier properties, Polym. Int. 63 (9) (Sep. 2014) 1620–1626, https://doi.org/10.1002/PI.4662.

[24] M.N. Ismail, N. Rafidi, R.J. Awale, and F. Ali, "Preparation and characterization of polylacticacid based polyurethane for environmental friendly packaging materials," *J. Adv. Res. Fluid Mech. Therm. Sci.*, vol. 38, no. 1, pp. 16–21, Oct. 2017, Accessed: Aug. 25, 2024. [Online]. Available: ⟨https://semarakilmu.com.my/journals/index.php/fluid_mechanics_thermal_sciences/article/view/2629⟩.

[25] E.K. Sitepu, et al., Microwave-assisted enzymatic esterification production of emollient esters, ACS Omega 8 (42) (Oct. 2023) 39168–39173, https://doi.org/10.1021/ACSOMEGA.3C04336/SUPPL_FILE/AO3C04336_SI_001.PDF.

[26] S.P. Dubey, et al., Microwave energy assisted synthesis of poly lactic acid via continuous reactive extrusion: modelling of reaction kinetics, RSC Adv. 7 (30) (Mar. 2017) 18529–18538, https://doi.org/10.1039/C6RA26514F.

[27] E. Gabano, M. Ravera, Microwave-assisted synthesis: can transition metal complexes take advantage of this 'green' method? Mol. 2022, Vol. 27, Page 4249 27 (13) (Jun. 2022) 4249, https://doi.org/10.3390/MOLECULES27134249.

[28] B. Kost, et al., The influence of the functional end groups on the properties of polylactide-based materials, Prog. Polym. Sci. 130 (7) (Jul. 2022), https://doi.org/10.1016/J.PROGPOLYMSCI.2022.101556.

[29] Y. Deng, et al., Experimental and DFT studies on electrochemical performances of ester-containing vinylimidazolium ionic liquids: effect of the ester substituent and anion, J. Chem. Eng. Data 68 (4) (Apr. 2023) 835–847, https://doi.org/10.1021/ACS.JCED.2C00729/SUPPL_FILE/JE2C00729_SI_001.PDF.

[30] V.C. Pierre, J.L. Pasek-Allen, R.K. Wilharm, J.C. Bischof, "NMR characterization of polyethylene glycol conjugates for nanoparticle functionalization,", ACS Omega 8 (4) (Jan. 2023) 4331–4336, https://doi.org/10.1021/ACSOMEGA.2C07669/ASSET/IMAGES/LARGE/AO2C07669_0007.JPEG.

[31] F.M. Lamberti, A. Ingram, J. Wood, Synergistic dual catalytic system and kinetics for the alcoholysis of poly(Lactic Acid), Process. 2021, Vol. 9, Page 921 9 (6) (May 2021) 921, https://doi.org/10.3390/PR9060921.

[32] É. Casey, R. Breen, G. Pareras, A. Rimola, J.D. Holmes, G. Collins, Guanidine functionalized porous SiO2 as heterogeneous catalysts for microwave depolymerization of PET and PLA, RSC Sustain 2 (4) (Apr. 2024) 1040–1051, https://doi.org/10.1039/D3SU00425B.

[33] A.A. Crook, R. Powers, Quantitative NMR-based biomedical metabolomics: current status and applications, Molecules 25 (21) (Nov. 2020) 5128, https://doi.org/10.3390/MOLECULES25215128.

[34] M. Massonie, C. Pinese, M. Simon, A. Bethry, B. Nottelet, X. Garric, Biodegradable tyramine functional gelatin/6 arms-PLA inks compatible with 3D two photon-polymerization printing and meniscus tissue regeneration, Biomacromolecules 25 (8) (Aug. 2024) 5098–5109, https://doi.org/10.1021/ACS.BIOMAC.4C00495.

[35] H.M. Dou, J.H. Ding, H. Chen, Z. Wang, A.F. Zhang, H.Bin Yu, Bio-based, biodegradable and amorphous polyurethanes with shape memory behavior at body temperature, RSC Adv. 9 (23) (Apr. 2019) 13104–13111, https://doi.org/10.1039/C9RA01583C.

[36] A.A. Amusa, A.L. Ahmad, Enhanced gas separation prowess using functionalized lignin-free lignocellulosic biomass / polysulfone composite membranes, Membr. (Basel) 11 (3) (2021) 202.

[37] A.B.D. Nandiyanto, R. Ragadhita, M. Fiandini, Interpretation of fourier transform infrared spectra (FTIR): a practical approach in the polymer/plastic thermal decomposition, Indones. J. Sci. Technol. 8 (1) (2023) 113–126, https://doi.org/10.17509/ijost.v8i1.53297.

[38] K. Sensui, T. Tarui, T. Miyamae, C. Sato, C. Sato, Evidence of chemical-bond formation at the interface between an epoxy polymer and an isocyanate primer, Chem. Commun. 55 (98) (Dec. 2019) 14833–14836, https://doi.org/10.1039/C9CC05911C.

[39] J. Reignier, F. Méchin, A. Sarbu, Chemical gradients in PIR foams as probed by ATR-FTIR analysis and consequences on fire resistance, Polym. Test. 93 (1) (Jan. 2021) 106972, https://doi.org/10.1016/J.POLYMERTESTING.2020.106972.

[40] W. Siriprom, N. Sangwaranatee, Herman, K. Chantarasunthon, K. Teanchai, N. Chamchoi, Characterization and analyzation of the poly (L-lactic acid) (PLA) films, Mater. Today Proc. 5 (7) (Jan. 2018) 14803–14806, https://doi.org/10.1016/J.MATPR.2018.04.009.

[41] M. Grabowski, B. Kost, A. Bodzioch, M. Bednarek, Functionalization of polylactide with multiple tetraphenylethane inifer groups to form PLA block copolymers with vinyl monomers, Int. J. Mol. Sci. 24 (1) (Jan. 2023) 19, https://doi.org/10.3390/IJMS24010019/S1.

[42] Y. Dulyanska, L. Cruz-Lopes, B. Esteves, R. Guiné, I. Domingos, "FTIR monitoring of polyurethane foams derived from acid-liquefied and base-liquefied polyols,", Polym. (Basel) 16 (15) (Aug. 2024) 2214, https://doi.org/10.3390/POLYM16152214/S1.

[43] T. Stern, Single-step synthesis and characterization of non-linear tough and strong segmented polyurethane elastomer consisting of very short hard and soft segments and hierarchical side-reacted networks and single-step synthesis of hierarchical hyper-branched poly, Mol. 2024, Vol. 29, Page 1420 29 (7) (Mar. 2024) 1420, https://doi.org/10.3390/MOLECULES29071420.

[44] P. Jutrzenka Trzebiatowska, A. Santamaria Echart, T. Calvo Correas, A. Eceiza, J. Datta, The changes of crosslink density of polyurethanes synthesised with using recycled component. Chemical structure and mechanical properties investigations, Prog. Org. Coat. 115 (2) (Feb. 2018) 41–48, https://doi.org/10.1016/J.PORGCOAT.2017.11.008.

[45] R. Guo, et al., Extremely strong and tough biodegradable poly(urethane) elastomers with unprecedented crack tolerance via hierarchical hydrogen-bonding interactions, Adv. Mater. 35 (21) (May 2023) 2212130, https://doi.org/10.1002/ADMA.202212130.

[46] C. Xu, Y. Hong, Rational design of biodegradable thermoplastic polyurethanes for tissue repair, Bioact. Mater. 15 (8) (Sep. 2022) 250–271, https://doi.org/10.1016/J.BIOACTMAT.2021.11.029.

[47] B. Du, et al., A waterborne polyurethane 3D scaffold containing PLGA with a controllable degradation rate and an anti-inflammatory effect for potential applications in neural tissue repair, J. Mater. Chem. B 8 (20) (May 2020) 4434–4446, https://doi.org/10.1039/D0TB00656D.

[48] Y. Zhou, F. Wu, L. Zhu, Z. Geng, R. Yang, J. Zhai, Synergistic effect of covalent cross-linking and physical hydrogen bonding associations on the mechanical properties of polyurethane thermoset elastomers, J. Appl. Polym. Sci. 141 (42) (Nov. 2024) e56114, https://doi.org/10.1002/APP.56114.

[49] M. Das, A.R. Parathodika, P. Maji, K. Naskar, Dynamic chemistry: the next generation platform for various elastomers and their mechanical properties with self-healing performance, Eur. Polym. J. 186 (3) (Mar. 2023) 111844, https://doi.org/10.1016/J.EURPOLYMJ.2023.111844.

[50] W. Ziegler, et al., Influence of different polyol segments on the crystallisation behavior of polyurethane elastomers measured with DSC and DMA experiments, Polym. Test. 71 (10) (Oct. 2018) 18–26, https://doi.org/10.1016/J.POLYMERTESTING.2018.08.021.

[51] J. Shi, et al., Tuning the flexibility and thermal storage capacity of solid–solid phase change materials towards wearable applications, J. Mater. Chem. A 8 (38) (Oct. 2020) 20133–20140, https://doi.org/10.1039/C9TA13925G.

[52] P. Król, B. Uram, K. Król, M. Pielichowska, Sochacka-Piętal, M. Walczak, "Synthesis and property of polyurethane elastomer for biomedical applications based on nonaromatic isocyanates, polyesters, and ethylene glycol,", Colloid Polym. Sci. 298 (8) (Aug. 2020) 1077–1093, https://doi.org/10.1007/S00396-020-04667-8/TABLES/7.

[53] D. Li, et al., Synthesis, structure, properties, and applications of fluorinated polyurethane, Polym. (Basel) 16 (7) (Apr. 2024) 959, https://doi.org/10.3390/POLYM16070959.

[54] H. Duan, J. Zhao, S. Li, D. Qi, J. Li, Flexible anti-counterfeiting circularly polarized luminescent elastomer from supramolecular polyurethanes, Adv. Opt. Mater. 12 (20) (Jul. 2024) 2400379, https://doi.org/10.1002/ADOM.202400379.

[55] S. Oprea, D. Timpu, V. Oprea, Design-properties relationships of polyurethanes elastomers depending on different chain extenders structures, J. Polym. Res. 26 (5) (May 2019) 1–15, https://doi.org/10.1007/S10965-019-1777-6/METRICS.

[56] M. Sáenz-Pérez, E. Lizundia, J.M. Laza, J. García-Barrasa, J.L. Vilas, L.M. León, Methylene diphenyl diisocyanate (MDI) and toluene diisocyanate (TDI) based polyurethanes: thermal, shape-memory and mechanical behavior, RSC Adv. 6 (73) (Jul. 2016) 69094–69102, https://doi.org/10.1039/C6RA13492K.

[57] T. Allami, A. Alamiery, M.H. Nassir, A.H. Kadhum, Investigating physio-thermo-mechanical properties of polyurethane and thermoplastics nanocomposite in various applications, Polym. (Basel) 13 (15) (Aug. 2021) 2467, https://doi.org/10.3390/POLYM13152467.

[58] D.S.W. Pau, C.M. Fleischmann, M.A. Delichatsios, Thermal decomposition of flexible polyurethane foams in air, Fire Saf. J. 111 (1) (Jan. 2020) 102925, https://doi.org/10.1016/J.FIRESAF.2019.102925.

[59] B.X. Cheng, et al., A review of microphase separation of polyurethane: characterization and applications, Polym. Test. 107 (3) (Mar. 2022) 107489, https://doi.org/10.1016/J.POLYMERTESTING.2022.107489.

[60] P. Somdee, T. Lassú-Kuknyó, C. Kónya, T. Szabó, K. Marossy, "Thermal analysis of polyurethane elastomers matrix with different chain extender contents for thermal conductive application,", J. Therm. Anal. Calorim. 138 (2) (Oct. 2019) 1003–1010, https://doi.org/10.1007/S10973-019-08183-Y/FIGURES/6.

[61] H. Dai, R. Hong, Y. Ma, X. Cheng, W. Zhang, A subtle change in the flexible achiral spacer does matter in supramolecular chirality: two-fold odd-even effect in polymer assemblies, Angew. Chem. Int. Ed. 62 (50) (Dec. 2023) e202314848, https://doi.org/10.1002/ANIE.202314848.

[62] A. Mouren, E. Pollet, L. Avérous, UV-curable aromatic polyurethanes from different sustainable resources: protocatechuic and cinnamic acids, Eur. Polym. J. 220 (Nov. 2024) 113481, https://doi.org/10.1016/J.EURPOLYMJ.2024.113481.

[63] N.Y. Akhanova, et al., Influence of fullerene content on the properties of polyurethane resins: a study of rheology and thermal characteristics, Heliyon 10 (12) (Jun. 2024) e33282, https://doi.org/10.1016/J.HELIYON.2024.E33282.

[64] M. Mukhopadhyay, U. Biswas, N. Mandal, S. Misra, On the development of shear surface roughness, J. Geophys. Res. Solid Earth 124 (2) (Feb. 2019) 1273–1293, https://doi.org/10.1029/2018JB016677.

[65] J. Ochola, C. Hume, D. Bezuidenhout, Analysis of morphological properties of fibrous electrospun polyurethane grafts using image segmentation, J. Mech. Behav. Biomed. Mater. 155 (7) (Jul. 2024) 106573, https://doi.org/10.1016/J.JMBBM.2024.106573.

[66] C. Thiyagu, I. Manjubala, U. Narendrakumar, Thermal and morphological study of graphene based polyurethane composites, Mater. Today Proc. 45 (1) (Jan. 2021) 3982–3985, https://doi.org/10.1016/J.MATPR.2020.08.641.

[67] S.A.R. Naga, T.A. El-Sayed, "Fatigue failure in polymeric materials: insights from experimental testing,", J. Fail. Anal. Prev. 24 (2) (Apr. 2024) 922–935, https://doi.org/10.1007/S11668-024-01874-1/FIGURES/13.

[68] Z. Major, Methodology used for characterizing the fracture and fatigue behavior of thermoplastic elastomers, Adv. Polym. Sci. 286 (2020) 273–296, https://doi.org/10.1007/12_2020_81.

[69] A. Blazejczyk, Morphometric analysis of one-component polyurethane foams applicable in the building sector via X-ray computed microtomography, Mater. (Basel, Switz. 11 (9) (Sep. 2018) 1717, https://doi.org/10.3390/MA11091717.

[70] I. Łukaszewska, S. Lalik, A. Bukowczan, M. Marzec, K. Pielichowski, K. N. Raftopoulos, Tailoring the physical properties of non-isocyanate polyurethanes by introducing secondary amino groups along their main chain, J. Mol. Liq. 391 (12) (Dec. 2023) 123263, https://doi.org/10.1016/J.MOLLIQ.2023.123263.

[71] Y. Swain, S.K. Badamali, Microwave assisted synthesis and spectroscopic characterisation of diphenyl carbonate functionalised nanoporous starch, J. Polym. Res. 27 (10) (Oct. 2020) 1–9, https://doi.org/10.1007/S10965-020-02277-0/METRICS.

[72] A. Gilet, et al., Unconventional media and technologies for starch etherification and esterification, Green. Chem. 20 (6) (Mar. 2018) 1152–1168, https://doi.org/10.1039/C7GC03135A.

[73] P. Kasprzyk, E. Sadowska, J. Datta, Investigation of thermoplastic polyurethanes synthesized via two different prepolymers, J. Polym. Environ. 27 (11) (Nov. 2019) 2588–2599, https://doi.org/10.1007/S10924-019-01543-7/FIGURES/8.

[74] H. Pan, et al., The effect of MDI on the structure and mechanical properties of poly (lactic acid) and poly(butylene adipate- co -butylene terephthalate) blends, RSC Adv. 8 (9) (Jan. 2018) 4610–4623, https://doi.org/10.1039/C7RA10745E.

[75] Y. Chen, et al., Effect of uniaxial pre-stretching on the microstructure and mechanical properties of poly[(ethylene oxide)-block-(amide-12)]-toughened poly (lactic acid) blend, RSC Adv. 7 (2) (Jan. 2017) 712–719, https://doi.org/10.1039/C6RA25729A.

[76] A.C. Ford, H. Gramling, S.C. Li, J.V. Sov, A. Srinivasan, L.A. Pruitt, Micromechanisms of fatigue crack growth in polycarbonate polyurethane: time dependent and hydration effects, J. Mech. Behav. Biomed. Mater. 79 (3) (Mar. 2018) 324–331, https://doi.org/10.1016/J.JMBBM.2018.01.008.

[77] J. Jeong, Y. Hong, M.W. Lee, M. Goh, Synthesis and enzymatic recycling of sugar-based bio-polyurethane foam, Eur. Polym. J. 171 (5) (May 2022) 111188, https://doi.org/10.1016/J.EURPOLYMJ.2022.111188.

[78] F. Xie, T. Zhang, P. Bryant, V. Kurusingal, J.M. Colwell, B. Laycock, Degradation and stabilization of polyurethane elastomers, Prog. Polym. Sci. 90 (3) (Mar. 2019) 211–268, https://doi.org/10.1016/J.PROGPOLYMSCI.2018.12.003.

[79] O. Trhlíková, et al., Microbial and abiotic degradation of fully aliphatic polyurethane foam suitable for biotechnologies, Polym. Degrad. Stab. 194 (12) (Dec. 2021) 109764, https://doi.org/10.1016/J.POLYMDEGRADSTAB.2021.109764.

[80] R. Wei, T. Tiso, J. Bertling, K. O'Connor, L.M. Blank, U.T. Bornscheuer, Possibilities and limitations of biotechnological plastic degradation and recycling, Nat. Catal. 2020 311 3 (11) (Oct. 2020) 867–871, https://doi.org/10.1038/s41929-020-00521-w.

[81] R. Meys, F. Frick, S. Westhues, A. Sternberg, J. Klankermayer, A. Bardow, Towards a circular economy for plastic packaging wastes – the environmental potential of chemical recycling, Resour. Conserv. Recycl. 162 (11) (Nov. 2020) 105010, https://doi.org/10.1016/J.RESCONREC.2020.105010.

[82] K. Skleničková, S. Abbrent, M. Halecký, V. Kočí, H. Beneš, Biodegradability and ecotoxicity of polyurethane foams: A review, Crit. Rev. Environ. Sci. Technol. 52 (2) (2022) 157–202, https://doi.org/10.1080/10643389.2020.1818496.

[83] J. Joseph, R.M. Patel, A. Wenham, J.R. Smith, Biomedical applications of polyurethane materials and coatings, Trans. IMF 96 (3) (May 2018) 121–129, https://doi.org/10.1080/00202967.2018.1450209.

[84] Q. Peng, et al., Direct polycondensation of l-lactic acid in hydrophobic bis (trifluoromethanesulfonyl)imide-anionic ionic liquids: a kinetic study, Eur. Polym. J. 158 (9) (Sep. 2021) 110692, https://doi.org/10.1016/J.EURPOLYMJ.2021.110692.

[85] J.O.C. de França, D. da Silva Valadares, M.F. Paiva, S.C.L. Dias, J.A. Dias, Polymers based on PLA from synthesis using D,L-Lactic Acid (or Racemic Lactide) and some biomedical applications: a short review, Polym. (Basel) 14 (12) (Jun. 2022) 2317, https://doi.org/10.3390/POLYM14122317.

[86] P.L. Yang, S.H. Tsai, K.N. Chen, D.S.H. Wong, A New Continuous flow microwave radiation process design for non-isocyanate polyurethane (NIPU), Polym. 2023,

[87] X. Zhao, H. Hu, X. Wang, X. Yu, W. Zhou, S. Peng, Super tough poly(lactic acid) blends: a comprehensive review, RSC Adv. 10 (22) (Apr. 2020) 13316–13368, https://doi.org/10.1039/D0RA01801E.

[88] E. Kabir, Application of microwave heating in polymer synthesis: a review, Results Chem. 6 (12) (Dec. 2023) 101178, https://doi.org/10.1016/J.RECHEM.2023.101178.

[89] H. Sardon, A.P. Dove, Plastics recycling with a difference, Sci. (80-.) 360 (6387) (Apr. 2018) 380–381, https://doi.org/10.1126/SCIENCE.AAT4997.

[90] J.V. Džunuzović, et al., Fabrication of polycaprolactone-based polyurethanes with enhanced thermal stability, Polym. 2024, Vol. 16, Page 1812 16 (13) (Jun. 2024) 1812, https://doi.org/10.3390/POLYM16131812.

[91] K.Y. Wong, M.R. Chia, G.B. Teh, S.W. Phang, S.N. Gan, S.L. Sin, Effect of halloysite nanoclay on the properties of castor oil–based polyurethane synthesized by microwave-assisted method, Mater. Perform. Charact. 13 (1) (Oct. 2024) 201–214, https://doi.org/10.1520/MPC20230123.

[92] A. Mouren, L. Avérous, Sustainable cycloaliphatic polyurethanes: from synthesis to applications, Chem. Soc. Rev. 52 (1) (Jan. 2023) 277–317, https://doi.org/10.1039/D2CS00509C.

[93] A. Das, P. Mahanwar, A brief discussion on advances in polyurethane applications, Adv. Ind. Eng. Polym. Res. 3 (3) (Jul. 2020) 93–101, https://doi.org/10.1016/J.AIEPR.2020.07.002.

Vol. 15, Page 2499 15 (11) (May 2023) 2499, https://doi.org/10.3390/POLYM15112499.